ISBN: 978-3-95450-232-5 ISSN: 2673-7000 doi:10.18429/JACoW-NAPAC2022-TUPA14

FAST FIRST-ORDER SPIN PROPAGATION FOR SPIN MATCHING AND POLARIZATION OPTIMIZATION WITH Bmad

J. M. Asimow, G. H. Hoffstaetter[1], D. Sagan, M. G. Signorelli, Cornell University, Ithaca, NY, USA
[1]also at Brookhaven National Laboratory, Upton, NY, USA

Abstract

Accurate spin tracking is essential for the simulation and propagation of polarized beams, in which a majority of the particles' spin point in the same direction. Bmad, an open-sourced library for the simulation of charged particle dynamics, traditionally tracks spin via integrating through each element of a lattice. While exceptionally accurate, this method has the drawback of being slow; at best, the runtime is proportional to the length of the element. By solving the spin transport equation for simple magnet elements, Bmad can reduce this algorithm to constant runtime while maintaining high accuracy. This method, known as "Sprint," enables quicker spin matching and prototyping of lattice designs via Bmad.

INTRODUCTION

The Thomas-BMT equation describes the way that a particle's spin is perturbed via magnetic fields. At every point in phase space, a particle's spin $\vec{S}$ precesses about the vector $\vec{\Omega}(z)$ according to the differential equation:

$$\frac{d\vec{S}}{ds} = \vec{\Omega}(z,s) \times \vec{S}. \tag{1}$$

Solutions to Eq. (1) are of the form $\vec{S}(s) = R(z,s)\vec{S}_0$, where R is a rotation matrix in $SO(3)$. One caveat is that the Bmad library uses quaternions to represent the net spin rotation, rather than matrices. Quaternions are a noncommutative associative extension of the imaginary numbers that follow the rule $\mathbf{i}^2 = \mathbf{j}^2 = \mathbf{k}^2 = \mathbf{ijk} = -1$. Quaternions need fewer computations than matrices to calculate a 3d rotation, and are thus preferable for computer applications. A quaternion rotation of angle θ about the unit vector $\vec{e} = e_x\hat{x} + e_y\hat{y} + e_z\hat{z}$ looks like:

$$q = \cos\left(\frac{\theta}{2}\right) + e_x \sin\left(\frac{\theta}{2}\right)\mathbf{i} + e_y \sin\left(\frac{\theta}{2}\right)\mathbf{j} + e_z \sin\left(\frac{\theta}{2}\right)\mathbf{k}\,. \tag{2}$$

The rotation resulting from two successive rotations q_0 and q_1 is described by the product $q_1 q_0$. Equation (1) describe an infinitesimal rotation around the vector $\vec{\Omega}$ by the angle $|\vec{\Omega}|ds$. The quaternion characterizing this rotation is therefore $dQ = 1 + ds\frac{1}{2}(\Omega_x\mathbf{i} + \Omega_y\mathbf{j} + \Omega_z\mathbf{k})$ [1]. The total rotation $q(s)$ then changes along s with the differential equation:

$$\frac{dq}{ds} = \frac{1}{2}\Omega q\,, \quad \Omega = \Omega_x\mathbf{i} + \Omega_y\mathbf{j} + \Omega_z\mathbf{k}\,. \tag{3}$$

Bmad can compute quaternions by numerically integrating Eq. (3) via interfacing with Etienne Forest's PTC code [2]. However, if Eq. (3) is linearized with respect to the phase space deviations from the accelerator's design orbit, one can compute the quaternions analytically for the typical magnet types. To do so, we split $\vec{\Omega}$ into a constant term $\vec{\Omega}_0$ and a first-order term $\vec{\omega}$ [3]. With g as the bend strength, k_1 as the quadrupole strength, and k_s as the solenoid strength, this Ω is

$$\Omega_{0x} = 0 \tag{4a}$$
$$\Omega_{0y} = -a\gamma g \tag{4b}$$
$$\Omega_{0s} = -(1+a)\,k_s \tag{4c}$$

$$\omega_x = \left[(1+a\gamma)\left(-k_1 y + \frac{1}{2}k_s' x\right) + (a\gamma - a)\,k_s x'\right] \tag{5a}$$
$$\omega_y = \left[(1+a\gamma)\left(-g^2 x - k_1 x + \frac{1}{2}k_s' y\right) + (a\gamma - a)\,k_s y' + \left(1 + \frac{a}{\gamma}\right) g\delta\right] \tag{5b}$$
$$\omega_s = \left[(1+a\gamma)\,(-g' y + k_s\delta) + (a\gamma - a)\,(g y' + g' y - k_s\delta)\right]. \tag{5c}$$

On the design orbit, the rotation resembles simple harmonic precession about $\vec{\Omega}_0$. Denoting this 0th order solution by the quaternion q_0, we write the full solution as $q = (q_0 + \Delta q) = q_0\,(1 + \Delta b)$, with $\Delta b = \frac{\Delta q}{q_0}$. Equation (3),

$$\frac{d}{ds}(q_0\,(1+\Delta b)) = \frac{1}{2}\Omega q \tag{6}$$

leads to the zeroth and first order expansions:

$$q_0' = \frac{1}{2}\Omega_0 q_0\,, \quad q_0'\Delta b + q_0\Delta b' = \frac{1}{2}\Omega_0\Delta b + \frac{1}{2}\omega q_0 \tag{7}$$

leading to:

$$\Delta b' = \frac{1}{2}q_0^{-1}\omega q_0\,. \tag{8}$$

For the linear phase space function ω in Eq. (5), Δb was integrated analytically.

Fringes were approximated using a hard-edge model, such that the fringe strength approaches a Dirac-Delta function. Misalignments were handled by shifting the center of the Taylor map, such that the constant term of the series includes the contributions from the misalignment.

ISBN: 978-3-95450-232-5 ISSN: 2673-7000 doi:10.18429/JACoW-NAPAC2022-TUPA14

COMPARISONS WITH PTC

Figure 1 shows comparisons between PTC and the method implemented by this paper ("Sprint") for equilibrium polarization P_{eq}, and the time to reach this equilibrium τ_{dk}.

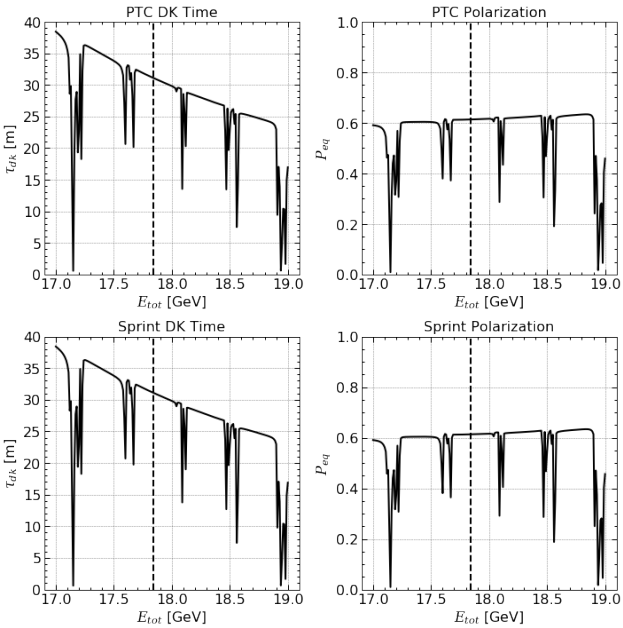

Figure 1: Polarization comparisons between Sprint and PTC on an EIC ESR 5.3 lattice, calculated via Bmad. PTC produces the data for this plot in roughly 2 hours, while Sprint produces the data in 20 minutes.

CONCLUSION

Bmad now supports quick calculations of spin polarization and propagation for all basic magnet elements. These results can be used for quick calculations of polarization limits and rates, and improve Bmad's capabilities for spin matching. Spin matching can be performed by converting a calculated quaternion into a 2x6 G-matrix and reducing the value of $\frac{\partial \hat{n}}{\partial \gamma}$ [2, 4]. The user can choose tracking method on an element by element basis, so that more accurate results can be obtained if deemed necessary.

APPENDIX

Tables 1-5 show the unnormalized calculated quaternions $q = q_0 + q_x\mathbf{i} + q_y\mathbf{j} + q_z\mathbf{k}$ for basic magnet elements. To calculate the exit fringe in Table 2, multiply all field strengths g by -1 and replace all entrance face angles e_1 with exit face angles $-e_2$. To calculate the exit fringe in Table 4, multiply all field strengths k_s by -1. The negative exit face angle is used due to Bmad convention [2]. These calculations improve upon previous literature by including hard-edge fringe fields, as well as distinguishing between different quadrupole orientations [5, 6].

REFERENCES

[1] G. H. Hoffstaetter, *High energy polarized proton beams: a modern view*. New York, NY, USA: Springer Publishing, Tracts in Modern Physics, 2006. doi:10.1007/978-0-387-34754-7

[2] Bmad Manual, rev. Jul. 2022, https://www.classe.cornell.edu/bmad/manual.html

[3] M.G. Signorelli and G.H. Hoffstaetter, "Different forms of first order spin-orbit motion and their utility in spin matching in electron storage rings," Dec. 2021. doi:10.48550/arXiv:2112.07607

[4] A. W. Chao *et al.*, *Handbook of accelerator physics and engineering*, 1st edition, 3rd printing, Singapore: World Scientific, 2006.

[5] C. Weisbaecker, "Nichtlineare effekte der spindynamik in protonenbeschleunigern," Ph.D. thesis, Institut fur Angewandte Physik, Technische Universitat Darmstadt, Germany, 1998.

[6] A.W. Chao, "Evaluation of radiative spin polarization in an electron storage ring," *Nucl. Instr. Meth.*, vol. 180, pp. 29-36, 1981. doi:10.1016/0029-554X(81)90006-9

ISBN: 978-3-95450-232-5 ISSN: 2673-7000 doi:10.18429/JACoW-NAPAC2022-TUPA14

Table 1: Constants Used for Quaternions

$d = gl$	$e = agl\gamma$	$s = ak_s l$	$t = (1+a)k_s l$
$c_d = \cos(d)$	$s_{e2} = \sin(\frac{e}{2})$	$c_s = \cos(s)$	$c_t = \cos(t)$
$s_d = \sin(d)$	$c_{e2} = \cos(\frac{e}{2})$	$s_s = \sin(s)$	$s_{t2} = \sin(\frac{t}{2})$
$\chi = 1 + a\gamma$	$\zeta = \gamma - 1$	$\psi = \gamma^2 - 1$	$c_{t2} = \cos(\frac{t}{2})$

Table 2: Sbend Entrance Fringe

	q_0	q_x	q_y	q_z
1	1			
x			$\frac{1}{2}\chi g \tan(e_1)$	
y		$\frac{1}{2}(1+a)g\sin(e_1)$		$-\frac{1}{2}(1+a)g\cos(e_1)$

Table 3: Sbend Body with Overlayed Quadrupole

$k_x = k_1 + g^2$	$\alpha = 2(a^2g^2\gamma^2 + k_1)$
$\omega_x = \sqrt{\lvert k_x \rvert}$	$\beta = agk_1(\gamma\chi - \zeta)$
$\omega_y = \sqrt{\lvert k_1 \rvert}$	$\sigma = \omega_y(k_1 + ak_1\gamma + a^2g^2\zeta\gamma)$
	$\xi = \omega_y(k_1\chi + a^2g^2\zeta\gamma)$

$k_x > 0$	$k_x < 0$	$k_1 > 0$	$k_1 < 0$
$s_x = \sin(l\omega_x)$	$\sinh(l\omega_x)$	$s_y = \sinh(l\omega_y)$	$\sin(l\omega_y)$
$c_x = \cos(l\omega_x)$	$\cosh(l\omega_x)$	$c_y = \cosh(l\omega_y)$	$\cos(l\omega_y)$
$\tau_x = -1$	$+1$	$\tau_y = +1$	-1

	q_0	q_x	q_y	q_z
1	c_{e2}		$-s_{e2}$	
x	$\frac{-k_x\chi}{2\omega_x}s_x s_{e2}$		$\frac{-k_x\chi}{2\omega_x}s_x c_{e2}$	
p_x	$\frac{k_x\chi}{2\omega_x^2}\tau_x(1-c_x)s_{e2}$		$\frac{k_x\chi}{2\omega_x^2}\tau_x(1-c_x)c_{e2}$	
y		$\frac{-1}{\alpha}[\beta(1+c_y)s_{e2} + \tau_y\sigma s_y c_{e2}]$		$\frac{1}{\alpha}[\beta(1-c_y)c_{e2} + \tau_y\sigma s_y s_{e2}]$
p_y		$\frac{1}{\omega_y\alpha}[\xi(1-c_y)c_{e2} - \beta s_y s_{e2}]$		$\frac{1}{\omega_y\alpha}[\xi(1+c_y)s_{e2} - \beta s_y c_{e2}]$
p_z	$\frac{g}{2}\left(\frac{\chi s_x}{\omega_x} - \frac{al\psi}{\gamma}\right)s_{e2}$		$\frac{g}{2}\left(\frac{\chi s_x}{\omega_x} - \frac{al\psi}{\gamma}\right)c_{e2}$	

Table 4: Solenoid Entrance Fringe

	q_0	q_x	q_y
1	1		
x		$\frac{1}{4}k_s\chi$	
y			$\frac{1}{4}k_s\chi$

Table 5: Solenoid Element Body

	q_0	q_x	q_y	q_z
1	c_{t2}			$-s_{t2}$
x		$\frac{1}{4}k_s\zeta((1-c_s)c_{t2} - s_s s_{t2})$	$\frac{1}{4}k_s\zeta((-1+c_s)s_{t2} - s_s c_{t2})$	
p_x		$\frac{1}{2}\zeta((1-c_s)st2 + s_s c_{t2})$	$\frac{1}{2}\zeta((1-c_s)c_{t2} - s_s s_{t2})$	
y		$\frac{1}{4}k_s\zeta((1-c_s)s_{t2} + s_s c_{t2})$	$\frac{1}{4}k_s\zeta((1-c_s)c_{t2} - s_s s_{t2})$	
p_y		$\frac{1}{2}\zeta((-1+c_s)c_{t2} + s_s s_{t2})$	$\frac{1}{2}\zeta((1-c_s)s_{t2} + s_s c_{t2})$	
p_z	$\frac{1}{2}ts_{t2}$			$\frac{1}{2}tc_{t2}$